JACS
JOURNAL OF THE AMERICAN CHEMICAL SOCIETY
Article
pubs.acs.org/JACS

New Mechanistic Pathways for Criegee–Water Chemistry at the Air/Water Interface

Chongqin Zhu,[†,‡] Manoj Kumar,[†] Jie Zhong,[†] Lei Li,[†] Joseph S. Francisco,*[,†] and Xiao Cheng Zeng*[,†,‡]

[†]Department of Chemistry, University of Nebraska—Lincoln, Lincoln, Nebraska 68588, United States

[‡]Beijing Advanced Innovation Center for Soft Matter Science and Engineering, Beijing University of Chemical Technology, Beijing 100029, China

Supporting Information

ABSTRACT: Understanding Criegee chemistry has become one of central topics in atmospheric research recently. The reaction of Criegee intermediates with gas-phase water clusters has been widely viewed as a key Criegee reaction in the troposphere. However, the effect of aerosols or clouds on Criegee chemistry has received little attention. In this work, we have investigated the reaction between the smallest Criegee intermediate, CH_2OO, and water clusters in the gas phase, as well as at the air/water surface using ab initio quantum chemical calculations and adaptive buffered force quantum mechanics/molecular mechanics (QM/MM) dynamics simulations. Our simulation results show that the typical time scale for the reaction of CH_2OO with water at the air/water interface is on the order of a few picoseconds, 2–3 orders of magnitude shorter than that in the gas phase. Importantly, the adbf-QM/MM dynamics simulations suggest several reaction pathways for the CH_2OO + water reaction at the air/water interface, including the loop-structure-mediated mechanism and the stepwise mechanism. Contrary to the conventional gas-phase CH_2OO reaction, the loop-structure is not a prerequisite for the stepwise mechanism. For the latter, a water molecule and the CH_2OO at the air/water interface, upon their interaction, can result in the formation of $(H_3O)^+$ and $(OH)CH_2(OO)^-$. Thereafter, a hydrogen bond can be formed between $(H_3O)^+$ and the terminal oxygen atom of $(OH)CH_2(OO)^-$, leading to direct proton transfer and the formation of α-hydroxy methylperoxide, $HOCH_2OOH$. The mechanistic insights obtained from this simulation study should motivate future experimental studies of the effect of water clouds on Criegee chemistry.

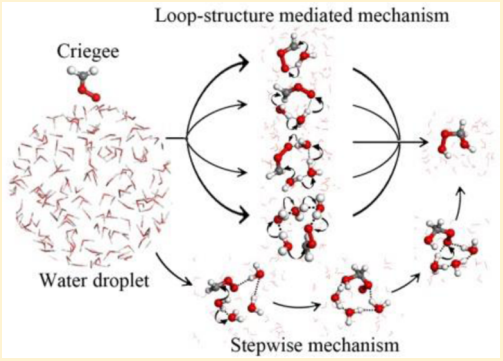

INTRODUCTION

Criegee intermediates are key branching points in the reactions between ozone and unsaturated hydrocarbons.[1] The unimolecular and bimolecular Criegee reactions directly lead to many end products important to atmospheric chemistry, such as hydroxyl radicals, organic acids, hydroperoxides, and aerosols.[2−5] The Criegee reactions that involve a number of atmospheric species (e.g., SO_2 and NO_2) are well documented in the literature.[6−10] However, noting that the concentration of water ($\sim 10^{23}$ m^{-3}) in the troposphere is orders of magnitude higher than that of atmospheric species like NO_2, SO_2 ($\sim 10^{18}$ m^{-3}), the impact of these oxidation reactions is determined by the reaction of Criegee intermediates with water.[11−13] Considering that the Criegee–water reaction is the most plausible reaction in the troposphere, it has been extensively investigated using various experimental and theoretical methods.[8,12−23] Most previous studies have focused on the reactions of Criegee intermediates with water monomer and/or dimer as shown in eqs 1 and 2:

$$(R_1)(R_2)COO + H_2O \rightarrow (R_1)(R_2)C(OH)OOH \quad (1)$$

$$(R_1)(R_2)COO + (H_2O)_2 \rightarrow (R_1)(R_2)C(OH)OOH + H_2O \quad (2)$$

It is known that the reaction between a Criegee intermediate and water vapor involves the *loop-structure mediated* mechanism.[21−25] Theoretical studies have shown that reaction 2 is more favored over reaction 1.[21,22] This has also been confirmed in recent experiments by Berndt et al.,[26] Chao et al.,[8] and Smith et al.[20] In these experiments, the second-order dependence of the Criegee loss on the concentration of water has been detected, indicating that reaction 2 predominates in the decay of CH_2OO in the atmospheric conditions. The reported rate coefficient for the reaction of the CH_2OO with water dimer is about $\sim 10^{-11}$ cm^3/s, significantly higher than that estimated for the reaction with water monomer ($\sim 10^{-16}$ cm^3/s) by Ouyang et al.[18] and Welz et al.[27] This discrepancy indicates that the reaction rate of CH_2OO with water vapor strongly depends on the water vapor concentration.[19] Many previous studies also show that aerosols, fog, and clouds may play a key role in atmospheric chemistry.[28−36] In the atmosphere, the abundance of aerosols can rise up to $\sim 10^8$–10^9 m^{-3}, and the maximum surface area of the aerosols in clouds can be $\sim 10^{-9}$ m^2.[37,38] These numbers suggest that the air/water interface can play a

Received: April 29, 2016
Published: August 10, 2016

DOI: 10.1021/jacs.6b04338
J. Am. Chem. Soc. 2016, 138, 11164–11169

more direct role in the Criegee−water reaction. On the other hand, a significant number of sulfate, nitrate, and organic compounds, which can react with CH_2OO, have been measured in aerosols and clouds,[30−33] which indicate that the reaction of CH_2OO with water at the air/water interface can assist in understanding oxidation reactions between CH_2OO and atmospheric species in aerosols. However, the effect of the air/water interface on the reaction of CH_2OO with water has yet to be examined.

In this paper, we show a direct evidence, on the basis of adaptive buffered force quantum mechanics/molecular mechanics (adbf-QM/MM) dynamics simulation, that the typical time scale for the reaction of the smallest Criegee intermediate, CH_2OO, with water at the air/water interface is about several picoseconds, 2−3 orders of magnitude shorter than that in the gas phase. The reaction between CH_2OO and water at the air/water surface can occur via multiple reaction pathways. In addition to the conventional loop-structure mediated mechanism, a two-step reaction pathway is identified for the first time for the CH_2OO−water reaction at the air/water interface. The feasibility of this new stepwise chemical mechanism suggests that the loop-structure is not the only pathway for the reaction between CH_2OO and water at the air/water interface. This result may aid in understanding the general effect of water droplet on the Criegee−water chemistry.

METHODS

The adbf-QM/MM[39] dynamics simulations were performed using the CP2K code.[40] Specifically, the QM (model) level of theory was the density functional theory within the formulation of the Becke−Lee−Yang−Parr (BLYP) exchange correlation functional[41,42] and with the DZVP basis set and Goedecker−Teter−Hutter (GTH) norm-conserved pseudopotentials.[43,44] The Grimme empirical van der Waals energy dispersion correction (D3) with a cutoff at 15 Å was applied.[45] In the MM model, the water molecules were described using the TIP3P model.[46] A box ($25 \times 25 \times 120$ Å^3) containing 495 water molecules and one Criegee molecule (CH_2OO) was employed (Figure S1a). Periodic boundary conditions were applied in the x and y directions (see the Supporting Information for more details of systems). The QM and buffer region selections are given in Table S1. All of the adbf-QM/MM simulations were carried out in the constant volume and temperature ensemble with the temperature controlled at 300 K using the massive Nose−Hoover−Langevin thermostats.[47] The time step of the adbf-QM/MM simulations is 1.0 fs. Constraints are applied to all bonds to hydrogen atoms using the SHAKE algorithm. Upon adsorption of a CH_2OO molecule onto the surface of the water, the system is further optimized prior to the adbf-QM/MM dynamics simulations. For each QM/MM simulation, it runs until the reaction occurs. To confirm the adbf-QM/MM results, ab initio molecular dynamics (AIMD) simulations are also performed for comparison. More details of computation methods are given in the Supporting Information.

RESULTS AND DISCUSSION

Gas-Phase Reaction. Prior to the adbf-QM/MM dynamics simulations, the climbing image nudged-elastic-band (CI-NEB) method is used to locate the transition state. In addition, high-level quantum chemical calculations are performed to confirm the gas-phase reactions of CH_2OO with water monomer and dimer (particularly the formation of loop-structure with the water dimer) at the CCSD(T)[48]/aug-cc-pVTZ[49]//M06-2X[50]/aug-cc-pVTZ level of theory implemented in the Gaussian09[51] software (see the Supporting Information). These independent high-level computations together with other high-level computations allow confirmation of the activation energy barrier for each reaction. The computed potential energy profiles for the gas-phase $CH_2OO + H_2O$ and the $CH_2OO + (H_2O)_2$ reactions are shown in Figure 1. The computed

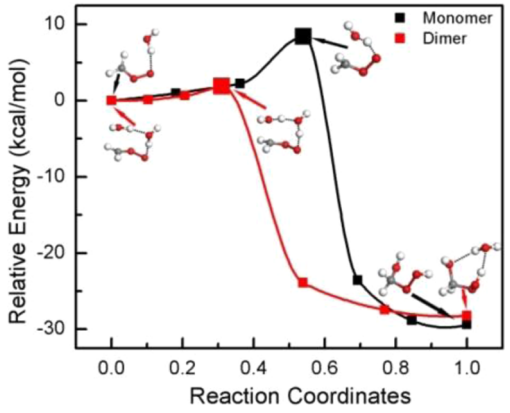

Figure 1. Schematic illustration of the energy profiles for the gas-phase reaction of CH_2OO with water monomer (black) and water dimer (red). The horizontal bar denotes the reactant or product state. The larger solid squares represent the transition states and smaller solid squares corresponding to the replicas in the climbing-image nudged elastic band (CI-NEB) method. The white, red, and gray spheres represent H, O, and C atoms, respectively.

reaction pathways for the $CH_2OO + H_2O$ and the $CH_2OO + (H_2O)_2$ reaction are consistent with those reported previously.[21−23] For the $CH_2OO + H_2O$ reaction, the computed activation barrier is 8.4 kcal/mol, in good agreement with theoretical calculations at higher levels of theory (7.6 kcal/mol at CCSD(T)/aug-cc-pVTZ//B3LYP/6-311+G(2df,2p)[52] and 9.2 kcal/mol at CCSD(T)/aug-cc-pVTZ//M06-2X/aug-cc-pVTZ level (Figure S2)). The HO fragment of H_2O binds to the Criegee carbon atom while its hydrogen atom adds to the terminal Criegee oxygen atom. This reaction results in the formation of α-hydroxy methylperoxide, $HOCH_2OOH$. In the $CH_2OO + (H_2O)_2$ reaction, the HO fragment of one water molecule binds to the Criegee carbon while the remnant hydrogen atom of the same water molecule gets concertedly attached to the other water molecule, which, in turn, gives its hydrogen atom to the terminal Criegee oxygen. Thus, the $CH_2OO + (H_2O)_2$ reaction can be viewed as the *water-mediated proton transfer* reaction. Indeed, the involvement of an additional water molecule facilitates the loop-structure formation around the reaction center and gives a relatively lower energy barrier of 1.9 kcal/mol than that for the water monomer reaction (2.2 kcal/mol at CCSD(T)/aug-cc-pVTZ//B3LYP/6-311+G(2df,2p)[52] and 3.2 kcal/mol at CCSD(T)/aug-cc-pVTZ//M06-2X/aug-cc-pVTZ level (Figure S2)).

Furthermore, 10 AIMD simulations are performed to examine the reaction of CH_2OO and water dimer in the gas phase. In our simulations, a supercell ($20 \times 20 \times 20$ Å^3) with periodic boundary conditions is selected for the (CH_2OO)-$(H_2O)_2$ system, which is large enough to neglect interaction between the neighboring replica. The initial structure of $(CH_2OO)(H_2O)_2$ system is optimized first (Figure S3), followed by the simulations of 80 ps (each). In these simulations, no reaction is observed, suggesting that the time scale for the reaction between CH_2OO and water dimer is likely beyond $\sim 10^2$ ps. This outcome is consistent with previous theoretical calculations (see below).[52] Anglada et al. used a

DOI: 10.1021/jacs.6b04338
J. Am. Chem. Soc. 2016, 138, 11164−11169

kinetic model to investigate the reaction between CH_2OO and water dimer, as shown in eq 3

$$CH_2OO + (H_2O)_2 \rightleftharpoons CH_2OO\cdots(H_2O)_2 \xrightarrow{k} HOCH_2OOH + H_2O \quad (3)$$

where k is the rate constant for the unimolecular isomerization of prereactive complex into the reaction product. Based on the highest k value ($\sim 10^9$ s^{-1} = 10^{-3} ps^{-1}) computed by Anglada et al. (see Table S4 in ref 52), the estimated shortest time scale for the $CH_2OO-(H_2O)_2$ reaction from the prereactive complex in gas phase is $\sim 10^3$ ps. Further, the calculations show that the effective rate for the reaction of CH_2OO with water dimer in the gas phase at temperature of 298 K and 20% relative humidity is $\sim 1.3 \times 10^4$ s^{-1}, about 2 orders of magnitude faster than that for the analogous water monomer reaction (5.5×10^2 s^{-1}).

Reaction at Air/Water Interface. Previous studies suggest that aerosols, fog, and cloudwater may play a key role in the atmospheric chemistry.[28−36,53] To gain deeper insights into the Criegee chemistry at the air/water interface, we carried out ten additional adbf-QM/MM dynamics simulations to study the mass accommodation of Criegee molecule on water surface (Figure S4; movie S1). No direct scattering of incoming Criegee molecules is observed, implying that the surface accommodation coefficient is nearly unity.

Next, 100 independent adbf-QM/MM dynamics simulations are carried out. Unlike the dimer system in the gas phase, the reaction of CH_2OO with water at the air/water interface can be directly observed during the adbf-QM/MM dynamics simulations. Figure 2 shows the fraction of CH_2OO unreacted

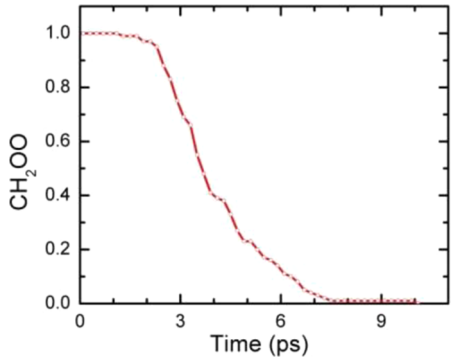

Figure 2. Fraction of CH_2OO unreacted versus time. One hundred independent adbf-QM/MM dynamics simulations were performed.

versus simulation time. All reactions occurred within 11 ps. The time scale for the reaction at the air/water interface is ~4.34 ps (within which 63% reactions are observed), which is 2−3 orders of magnitude shorter than that (10^2 to 10^3 ps) in the gas phase.

Loop-Structure-Mediated Reaction. Among these 100 simulations, 76 involve the loop-structure-mediated reactions. As shown in Figure 3a, the smallest looplike structure between CH_2OO and the water monomer is observed before the formation of final product, $HOCH_2OOH$ (movie S2). This event occurs at ~3.52 ps and results in the formation of an activated complex, where the C−O1 and the O2−H1 lengths decrease to ~1.50 and ~1.00 Å, respectively, confirming the formation of $HOCH_2OOH$ from the reaction of CH_2OO with water monomer (Figure 3e). For the water dimer, trimer, or tetramer reactions at the air/water interface, the larger loop-structures showing the activated complex formation between CH_2OO and water dimer, trimer, or tetramer were also observed within a few picoseconds (Figure 3b (movie S3), 3c (movie S4), and 3d (movie S5)). The shortening of the C−O1 and the O3−H2 (O4−H3 or O5−H4) length is also noticed during the water dimer (Figure 3f), trimer (Figure 3g), or tetramer (Figure 3h) reactions, indicative of the $HOCH_2OOH$ formation. An AIMD simulation is also performed, and the result confirms the loop-structure mediated reaction (see movie S6) predicted from the adbf-QM/MM dynamics simulation.

Population Analysis. Population analysis reveals that at the air/water interface and 300 K, nearly 76% of the CH_2OO−water reaction follows the loop-structure-mediated mechanism (Figure 4). In these loop-structure-mediated reactions, the obtained population value is the highest for the water dimer reaction: ~52%, whereas only ~5% of the Criegee reaction involves the water monomer. This suggests that at the air/water interface and 300 K, the water dimer forms a better proton loop-structure around the reaction center, which makes the CH_2OO−water dimer reaction thermodynamically more favorable than the CH_2OO−water monomer reaction, a mechanistic feature akin to the gas-phase reaction.

Stepwise Mechanism at the Air/Water Interface. In addition to the loop-structure-meditated concerted Criegee−water reactions, the stepwise reaction of CH_2OO with water at the air/water interface is also observed in one adbf-QM/MM dynamics simulation. Interestingly, this new chemical mechanism does not require the formation of the loop-structure (Figure 5). In the first step, the C−O1 length and the O2−H1 length are shortened to ~1.50 and ~1.06 Å, respectively, indicating the binding of the HO fragment of water to the Criegee carbon and the formation of $(H_3O)^+$ at ~1.10 ps (Figure 5a and movie S7). This leads to the breakage of the O1−H1 bond. Notably, the distance between the terminal Criegee oxygen (O3) and the other water hydrogen (H2) is appreciably large at this point (O3−H2 ~1.80 Å), suggesting that the water hydrogen does not bind to the terminal Criegee oxygen. In the next step, a ringlike structure involving $(H_3O)^+$, two water molecules, and the terminal oxygen atom of $(OH)CH_2(OO)^-$ is formed (Figure 5b). As shown in Figure 5d, the O1−H1 length decreases to ~1.06 Å, indicating the formation of the O1−H1 bond. The concerted breakage of O2−H1 bond is also observed in the simulation (lower panel, Figure 5d). An important mechanistic difference between the loop-structure-mediated proton-transfer mechanism and the stepwise one is that in the stepwise mechanism, a proton in $(H_3O)^+$ directly transfers to the terminal oxygen atom of $(OH)CH_2(OO)^-$ rather than through the water "bridge". To confirm the possibility of this two-step mechanism, the geometry of the intermediate formed after the initial OH addition to the Criegee intermediate at the air/water interface was optimized at the BLYP-D level, which is found to be stable (Figure S5). Note that ~24% of the CH_2OO−water reaction at the air/water interface follows the stepwise mechanism, which is even more than the fraction of the Criegee reaction involving water trimer (17%). These results show that the stepwise mechanism can play a key role in the Criegee−water reactions at the air/water interface. On the other hand, previous studies show that the energy barrier for the reactions of other Criegee intermediates with water dimer may be much higher, some even higher than the $CH_2OO + H_2O$ reaction.[52] For example, the energy barrier of *syn*-CH_3CHOO (*anti*-CH_3CHOO) +

DOI: 10.1021/jacs.6b04338
J. Am. Chem. Soc. 2016, 138, 11164−11169

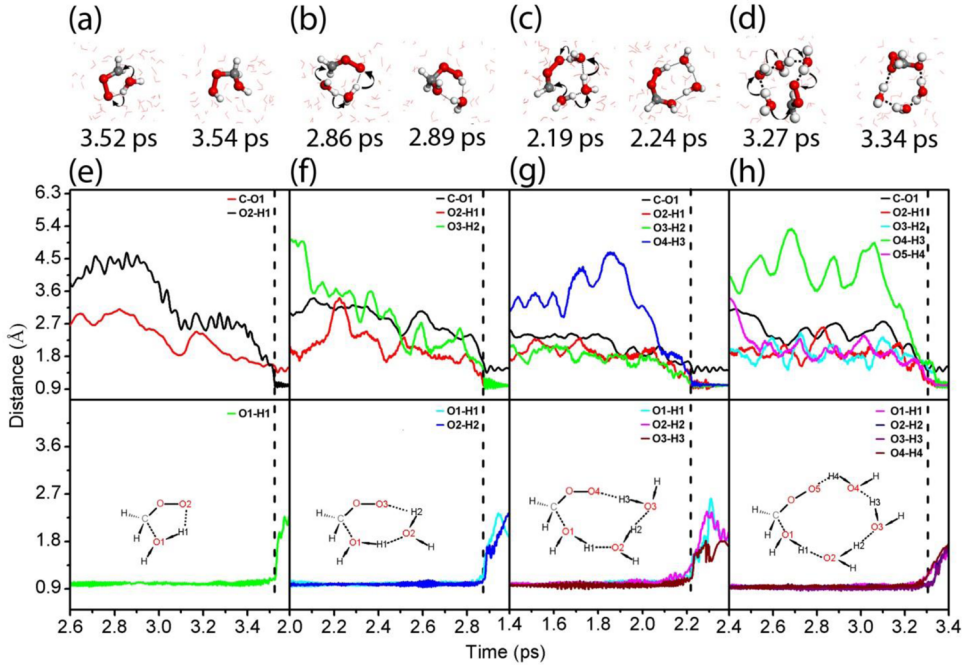

Figure 3. Snapshot structures taken from the abdf-QM/MM dynamics simulations of the reaction between CH_2OO and water monomer (a), water dimer (b), water trimer (c) and water tetramer (d), respectively. Corresponding time evolution of key bond distances is shown in (e), (f), (g), and (h), respectively. The insets illustrate the formation of the loop-structure in the activation complexes.

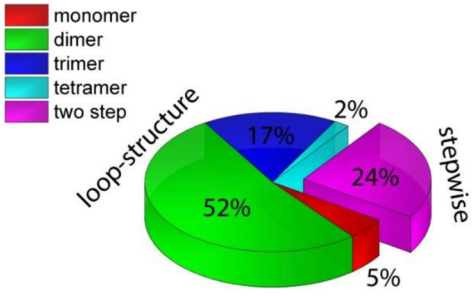

Figure 4. Adbf-QM/MM simulation based population analysis of the reaction of CH_2OO with water monomer (red), water dimer (green), water trimer (blue), and water tetramer (cyan), respectively, at the air/water interface. The fraction of the stepwise Criegee reaction is shown in magenta.

$(H_2O)_2$ reaction is ~6.0 kcal/mol (3.93 kcal/mol) at the CCSD(T)/aug-cc-pVTZ//B3LYP/6-311+G(2df,2p) level of theory. Thus, the stepwise mechanism may play even more important role in other Criegee intermediate water reactions at the air/water interface, especially for those Criegee intermediates, which react with water vapor relatively slowly.

CONCLUSIONS

In conclusion, we have demonstrated from direct adaptive buffered force QM/MM dynamics simulations that the time scale for the reaction of CH_2OO with water at the air/water interface and at 300 K is 2−3 orders of magnitude shorter than that in the gas phase. Importantly, the reaction of the smallest Criegee intermediate, CH_2OO, with water at the air/water surface occurs via both loop-structure-mediated and stepwise mechanisms. In the loop-structure-meditated reaction, the hydroxyl and hydrogen fragments of water directly bind to the Criegee carbon atom and terminal Criegee oxygen, respectively, while the other water molecules (if exist) serve

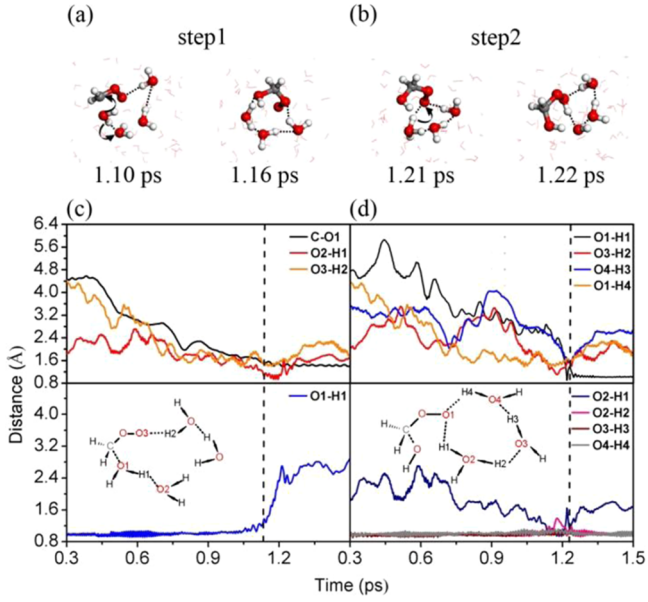

Figure 5. Snapshot structures taken from the QM/MM dynamics simulations of the two-step reaction of CH_2OO toward water. (a, b) First step and second step, respectively. (c, d) Time evolution of key bond distances involved in the first step and second step.

as a "bridge" to promote the proton transfer. Population analysis shows that the reaction of CH_2OO toward the water dimer is the dominant reaction pathway at the air/water interface, akin to the mechanistic feature predicted from the gas-phase calculations. At the air/water interface, an appreciable fraction of the CH_2OO reaction occurs via the two-step reaction mechanism. In this new mechanism, a water molecule first interacts with CH_2OO, leading to the formation of $(H_3O)^+$ and $(HO)CH_2(OO)^-$. Next, an H-bond is formed with $(H_3O)^+$ and the terminal oxygen atom of $(HO)CH_2(OO)^-$, which

DOI: 10.1021/jacs.6b04338
J. Am. Chem. Soc. 2016, 138, 11164−11169

facilitates subsequent direct proton transfer required for the formation of $HOCH_2OOH$. It is worth mentioning that in the stepwise mechanism, the formation of the loop-structure around the reaction center is not required. To our knowledge, the stepwise mechanism for the Criegee−water reaction at the air/water interface was not reported in the literature. The mechanistic insights obtained from our simulation study will promote future experimental studies of the effect of aerosols and clouds on Criegee chemistry and have important implications to the chemistry in the troposphere.

■ ASSOCIATED CONTENT

Supporting Information

Snapshot of Criegee intermediate at the air/water interface; parameters used in our adbf-QM/MM dynamical simulations; computation details of AIMD simulations; BLYP-D-optimized geometry of the intermediate formed in the first-step of the stepwise mechanism; videos of trajectories of the adbf-QM/MM simulations for the monomer, the dimer, the trimer and the two-step reactions at the air/water interface; M06-2X-optimized geometries of key stationary points for the gas-phase reactions of CH_2OO with water monomer and water dimer, respectively; and videos of trajectories of the AIMD simulation. The Supporting Information is available free of charge on the ACS Publications website at DOI: 10.1021/jacs.6b04338.

Trajectories of the adbf-QM/MM simulation for the mass accommodation of Criegee molecule on water surface (MPG)

Trajectories of the adbf-QM/MM simulation for the monomer at the air/water interface (MPG)

Trajectories of the adbf-QM/MM simulation for the dimer at the air/water interface (MPG)

Trajectories of the adbf-QM/MM simulation for the trimer at the air/water interface (MPG)

Trajectories of the adbf-QM/MM simulation for the tetramer at the air/water interface (MPG)

Trajectories of the AIMD simulation for the dimer at the air/water interface (MPG)

Trajectories of the adbf-QM/MM simulation for the two-step reactions at the air/water interface (MPG)

Trajectories of the adbf-QM/MM simulation for adsorption of a CH_2OO molecule onto the surface of the water droplet (MPG)

Snapshot of Criegee intermediate at the air/water interface; parameters used in our adbf-QM/MM dynamical simulations; computation details of AIMD simulations; BLYP-D-optimized geometry of the intermediate formed in the first step of the stepwise mechanism; M06-2X-optimized geometries of key stationary points for the gas-phase reactions of CH_2OO with water monomer and water dimer, respectively (PDF)

■ AUTHOR INFORMATION

Corresponding Authors

*jfrancisco3@unl.edu

*xzeng1@unl.edu

Notes

The authors declare no competing financial interest.

■ ACKNOWLEDGMENTS

We thank Professors Wenchuan Wang, Yixin Qu, and Daojian Cheng at BUCT for valuable discussions. This work is supported by the US National Science Foundation (CHE-1500217), by a fund from Beijing Advanced Innovation Center for Soft Matter Science & Engineering in BUCT for summer visiting scholar, and by the University of Nebraska Holland Computing Center.

■ REFERENCES

(1) Criegee, R. *Angew. Chem., Int. Ed. Engl.* **1975**, *14*, 745.

(2) Harrison, R. M.; Yin, J.; Tilling, R. M.; Cai, X.; Seakins, P. W.; Hopkins, J. R.; Lansley, D. L.; Lewis, A. C.; Hunter, M. C.; Heard, D. E.; Carpenter, L. J.; Creasey, D. J.; Lee, J. D.; Pilling, M. J.; Carslaw, N.; Emmerson, K. M.; Redington, A.; Derwent, R. G.; Ryall, D.; Mills, G.; Penkett, S. A. *Sci. Total Environ.* **2006**, *360*, 5.

(3) Emmerson, K. M.; Carslaw, N.; Carslaw, D. C.; Lee, J. D.; McFiggans, G.; Bloss, W. J.; Gravestock, T.; Heard, D. E.; Hopkins, J.; Ingham, T.; Pilling, M. J.; Smith, S. C.; Jacob, M.; Monks, P. S. *Atmos. Chem. Phys.* **2007**, *7*, 167.

(4) Stone, D.; Whalley, L. K.; Heard, D. E. *Chem. Soc. Rev.* **2012**, *41*, 6348.

(5) Kidwell, N. M.; Li, H.; Wang, X.; Bowman, J. M.; Lester, M. I. *Nat. Chem.* **2016**, *8*, 509.

(6) Osborn, D. L.; Taatjes, C. A. *Int. Rev. Phys. Chem.* **2015**, *34*, 309.

(7) Lee, Y. P. *J. Chem. Phys.* **2015**, *143*, 020901.

(8) Chao, W.; Hsieh, J. T.; Chang, C. H.; Lin, J. J. M. *Science* **2015**, *347*, 751.

(9) Lewis, T. R.; Blitz, M. A.; Heard, D. E.; Seakins, P. W. *Phys. Chem. Chem. Phys.* **2015**, *17*, 4859.

(10) Liu, F.; Fang, Y.; Kumar, M.; Thompson, W. H.; Lester, M. I. *Phys. Chem. Chem. Phys.* **2015**, *17*, 20490.

(11) Sarwar, G.; Simon, H.; Fahey, K.; Mathur, R.; Goliff, W. S.; Stockwell, W. R. *Atmos. Environ.* **2014**, *85*, 204.

(12) Sarwar, G.; Fahey, K.; Kwok, R.; Gilliam, R. C.; Roselle, S. J.; Mathur, R.; Xue, J.; Yu, J. Z.; Carter, W. P. L. *Atmos. Environ.* **2013**, *68*, 186.

(13) Li, J. Y.; Ying, Q.; Yi, B. Q.; Yang, P. *Atmos. Environ.* **2013**, *79*, 442.

(14) Stone, D.; Blitz, M.; Daubney, L.; Howes, N. U. M.; Seakins, P. *Phys. Chem. Chem. Phys.* **2014**, *16*, 1139.

(15) Suto, M.; Manzanares, E. R.; Lee, L. C. *Environ. Sci. Technol.* **1985**, *19*, 815.

(16) Becker, K. H.; Bechara, J.; Brockmann, K. J. *Atmos. Environ., Part A* **1993**, *27*, 57.

(17) Leather, K. E.; McGillen, M. R.; Cooke, M. C.; Utembe, S. R.; Archibald, A. T.; Jenkin, M. E.; Derwent, R. G.; Shallcross, D. E.; Percival, C. J. *Atmos. Chem. Phys.* **2012**, *12*, 469.

(18) Ouyang, B.; McLeod, M. W.; Jones, R. L.; Bloss, W. J. *Phys. Chem. Chem. Phys.* **2013**, *15*, 17070.

(19) Huang, H. L.; Chao, W.; Lin, J. J. M. *Proc. Natl. Acad. Sci. U. S. A.* **2015**, *112*, 10857.

(20) Smith, M. C.; Chang, C. H.; Chao, W.; Lin, L. C.; Takahashi, K.; Boering, K. A.; Lin, J. J. M. *J. Phys. Chem. Lett.* **2015**, *6*, 2708.

(21) Lin, L. C.; Chang, H. T.; Chang, C. H.; Chao, W.; Smith, M. C.; Chang, C. H.; Lin, J. J. M.; Takahashi, K. *Phys. Chem. Chem. Phys.* **2016**, *18*, 4557.

(22) Ryzhkov, A. B.; Ariya, P. A. *Chem. Phys. Lett.* **2003**, *367*, 423.

(23) Ryzhkov, A. B.; Ariya, P. A. *Phys. Chem. Chem. Phys.* **2004**, *6*, 5042.

(24) Newland, M. J.; Rickard, A. R.; Alam, M. S.; Vereecken, L.; Munoz, A.; Rodenas, M.; Bloss, W. J. *Phys. Chem. Chem. Phys.* **2015**, *17*, 4076.

(25) Long, B.; Tan, X. F.; Long, Z. W.; Wang, Y. B.; Ren, D. S.; Zhang, W. J. *J. Phys. Chem. A* **2011**, *115*, 6559.

(26) Berndt, T.; Voigtlander, J.; Stratmann, F.; Junninen, H.; Mauldin, R. L., III; Sipila, M.; Kulmala, M.; Herrmann, H. *Phys. Chem. Chem. Phys.* **2014**, *16*, 19130.

DOI: 10.1021/jacs.6b04338
J. Am. Chem. Soc. 2016, 138, 11164−11169

(27) Welz, O.; Savee, J. D.; Osborn, D. L.; Vasu, S. S.; Percival, C. J.; Shallcross, D. E.; Taatjes, C. A. *Science* **2012**, *335*, 204.
(28) Ravishankara, A. R. *Science* **1997**, *276*, 1058.
(29) Ravishankara, A. R.; Longfellow, C. A. *Phys. Chem. Chem. Phys.* **1999**, *1*, 5433.
(30) Monod, A.; Carlier, P. *Atmos. Environ.* **1999**, *33*, 4431.
(31) Blando, J. D.; Turpin, B. J. *Atmos. Environ.* **2000**, *34*, 1623.
(32) Jacob, D. J. *Atmos. Environ.* **2000**, *34*, 2131.
(33) Kolb, C. E.; Cox, R. A.; Abbatt, J. P. D.; Ammann, M.; Davis, E. J.; Donaldson, D. J.; Garrett, B. C.; George, C.; Griffiths, P. T.; Hanson, D. R.; Kulmala, M.; McFiggans, G.; Poschl, U.; Riipinen, I.; Rossi, M. J.; Rudich, Y.; Wagner, P. E.; Winkler, P. M.; Worsnop, D. R.; O' Dowd, C. D. *Atmos. Chem. Phys.* **2010**, *10*, 10561.
(34) Li, L.; Kumar, M.; Zhu, C. Q.; Zhong, J.; Francisco, J. S.; Zeng, X. C. *J. Am. Chem. Soc.* **2016**, *138*, 1816.
(35) Anglada, J. M.; Martins-Costa, M.; Ruiz-Lopez, M. F.; Francisco, J. S. *Proc. Natl. Acad. Sci. U. S. A.* **2014**, *111*, 11618.
(36) Zhong, J.; Zhao, Y.; Li, L.; Li, H.; Francisco, J. S.; Zeng, X. C. *J. Am. Chem. Soc.* **2015**, *137*, 12070.
(37) Gultepe, I.; Isaac, G. A. *Q. J. R. Meteorol. Soc.* **2004**, *130*, 2377.
(38) Guyon, P.; Graham, B.; Beck, J.; Boucher, O.; Gerasopoulos, E.; Mayol-Bracero, O. L.; Roberts, G. C.; Artaxo, P.; Andreae, M. O. *Atmos. Chem. Phys.* **2003**, *3*, 951.
(39) Bernstein, N.; Varnai, C.; Solt, I.; Winfield, S. A.; Payne, M. C.; Simon, I.; Fuxreiter, M.; Csanyi, G. *Phys. Chem. Chem. Phys.* **2012**, *14*, 646.
(40) VandeVondele, J.; Krack, M.; Mohamed, F.; Parrinello, M.; Chassaing, T.; Hutter, J. *Comput. Phys. Commun.* **2005**, *167*, 103.
(41) Becke, A. D. *Phys. Rev. A: At., Mol., Opt. Phys.* **1988**, *38*, 3098.
(42) Lee, C. T.; Yang, W. T.; Parr, R. G. *Phys. Rev. B: Condens. Matter Mater. Phys.* **1988**, *37*, 785.
(43) Hartwigsen, C.; Goedecker, S.; Hutter, J. *Phys. Rev. B: Condens. Matter Mater. Phys.* **1998**, *58*, 3641.
(44) Goedecker, S.; Teter, M.; Hutter, J. *Phys. Rev. B: Condens. Matter Mater. Phys.* **1996**, *54*, 1703.
(45) Grimme, S.; Antony, J.; Ehrlich, S.; Krieg, H. *J. Chem. Phys.* **2010**, *132*, 154104.
(46) Jorgensen, W. L.; Chandrasekhar, J.; Madura, J. D.; Impey, R. W.; Klein, M. L. *J. Chem. Phys.* **1983**, *79*, 926.
(47) Leimkuhler, B.; Noorizadeh, E.; Theil, F. *J. Stat. Phys.* **2009**, *135*, 261.
(48) Purvis, G. D.; Bartlett, R. J. *J. Chem. Phys.* **1982**, *76*, 1910.
(49) Dunning, T. H. *J. Chem. Phys.* **1989**, *90*, 1007.
(50) Zhao, Y.; Truhlar, D. G. *Theor. Chem. Acc.* **2008**, *120*, 215.
(51) Frisch, M. J.; Trucks, G. W., Schlegel, H. B.; Scuseria, G. E.; Robb, M. A.; Cheeseman, J. R.; Scalmani, G.; Barone, V.; Mennucci, B.; Petersson, G. A.; Nakatsuji, H.; Caricato, M.; Li, X.; Hratchian, H. P.; Izmaylov, A. F.; Bloino, J.; Zheng, G.; Sonnenberg, J. L.; Hada, M.; Ehara, M.; Toyota, K.; Fukuda, R.; Hasegawa, J.; Ishida, M.; Nakajima, T.; Honda, Y.; Kitao, O.; Nakai, H.; Vreven, T.; Montgomery, J. A., Jr.; Peralta, J. E.; Ogliaro, F.; Bearpark, M.; Heyd, J. J.; Brothers, E.; Kudin, K. N.; Staroverov, V. N.; Kobayashi, R.; Normand, J.; Raghavachari, K.; Rendell, A.; Burant, J. C.; Iyengar, S. S.; Tomasi, J.; Cossi, M.; Rega, N.; Millam, J. M.; Klene, M.; Knox, J. E.; Cross, J. B.; Bakken, V.; Adamo, C.; Jaramillo, J.; Gomperts, R.; Stratmann, R. E.; Yazyev, O.; Austin, A. J.; Cammi, R.; Pomelli, C.; Ochterski, J. W.; Martin, R. L.; Morokuma, K.; Zakrzewski, V. G.; Voth, G. A.; Salvador, P.; Dannenberg, J. J.; Dapprich, S.; Daniels, A. D.; Farkas, Ö.; Foresman, J. B.; Ortiz, J. V.; Cioslowski, J.; Fox, D. J. *Gaussian 09*; Gaussian, Inc.: Wallingford, CT, 2009.
(52) Anglada, J. M.; Sole, A. *Phys. Chem. Chem. Phys.* **2016**, *18*, 17698.
(53) Martins-Costa, M. T. C.; Anglada, J. M.; Francisco, J. S.; Ruiz-Lopez, M. F. *J. Am. Chem. Soc.* **2012**, *134*, 11821.

DOI: 10.1021/jacs.6b04338
J. Am. Chem. Soc. 2016, 138, 11164−11169